University of Stavanger

Faculty of Science and Technology

MASTER'S THESIS

Study program/ Specialization: Engineering structures and materials	Spring semester, 2020 Open / ~~Restricted access~~
Writer: Olav Kleppa	(Writer's signature)

Faculty supervisor:

Dr. Charlotte Obhrai

Thesis title:

Comparison of weather data from FINO3 and ERA5 in Wind Farm Installation Campaign Simulations.

Credits (ECTS): 30

Key words: Offshore Wind; Wind Farm; ERA5; Installation Campaign; FINO; Waiting on Weather

Pages: 47

+ enclosure: 51

Stavanger, 30/6-2020

Date/year

Abstract

Weather data are commonly used in the planning phase of an offshore wind farm installation campaign. Knowledge of site-specific weather conditions is of great importance regarding transport and installation as well as potential performance of the wind farm.
When observational data are not accessible for the location of interest, the data can be obtained from a forecast based on models and observations.
In this study a comparison is made between observational weather data from the FINO3 research facility and weather data from the global ERA5 climate reanalysis at matching location for the period 1.10.2013-30.09.2019.
The data from both sources was collected, filtered and matched with respect to time. A comparison was done between wind speed at 100-meter altitude as well as the wave height, also addressing the uncertainties associated with the ERA5 reanalysis.

A simulation was conducted using the intelligent simulation tool SIMSTALL from Shoreline to address the project installation time and accumulated waiting on weather for a hypothetical wind farm using weather data input from FINO3 and ERA5.

It was found that though the wind speed data from the ERA5 reanalysis on average was slightly higher than observations from FINO3, the number of available wind weather windows for the installation processes was higher in the ERA5 dataset.
For the wave height data, the ERA5 reanalysis showed a small underestimation compared to observational data. This led to a higher number of wave weather windows in the ERA5 dataset.
For the total installation time of the fictive wind farm created, the use of ERA5 weather data led to a month earlier completion as an average of twelve different starting months compared to using the observational data from FINO3, with a completion time of 534 days using ERA5 weather data and 564 days using FINO3 weather data.

Acknowledgement

My supervisor for this project was Dr. Charlotte Obhrai.

I would like to thank Ole-Erik V. Endrerud for granting access to the Shoreline simulation tool used in this study, and Oyegbile Afolarinwa David for sharing his experiences using this software.

Michela Giusti and Paul Berrisford from Copernicus ECMWF user support provided valuable help and inputs throughout the process.

Table of contents

Symbols and abbreviations

Abbreviations

IEA	International Energy Agency
ERA	ECMWF Re-Analysis
ECMWF	European Centre for Medium-Range Weather Forecasts
FINO	Forschungsplattformen in Nord- und Ostsee (1, 2 and 3).
NVE	Norges vassdrags- og energidirektorat
CDS	Climate Data Store
NetCDF	Network Common Data Form
EPS	Ensemble Prediction System
IFS	Integrated Forecast System
AWoW	Accumulated Waiting on Weather
ENS	Ensemble
RMS	Root Mean Square

Symbols

°	Degree, angular
U	Wind speed
u	Eastward component of wind
v	Northward component of wind
z_{hub}	Hub height
Z	Reference height
U_{hub}	Wind speed at hub height
α	Power law coefficient

List of figures

List of tables

1 introduction

In the Paris Agreement, an International climate policy agreement originally signed by 175 countries worldwide, it is decided to minimize emission of greenhouse gasses and limit the global warming to a maximum of 2 degrees, preferably 1,5 compared to the pre-industrial time period (Jakobsen & Kallbekken, 2020).

Transition to renewable sources of energy is a major factor in this regard, and wind power could possibly be a great potential for Norwegian energy production in the future.

Since wind has a higher energy potential offshore compared to onshore, in combination with challenges associated with obtaining areas for wind farm installations onshore, offshore wind power is considered a great potential.

The IEA estimates that offshore wind power can cover as much as 20% of the electricity production in Europe by 2040, becoming the largest source of electric power in Europe (IEA, 2019). Norway has a continental shelf of over 2 million square kilometres, or approximately six times the land area of mainland Norway. These areas offer a high potential of wind energy, though mainly in deeper water requiring floating turbines.

Figure 1 illustrates the wind potential offshore and onshore in Norway by colours indicating annually averaged windspeeds at 80 m altitude (Byrkjedal, Åkervik, & Vindteknikk, 2009):

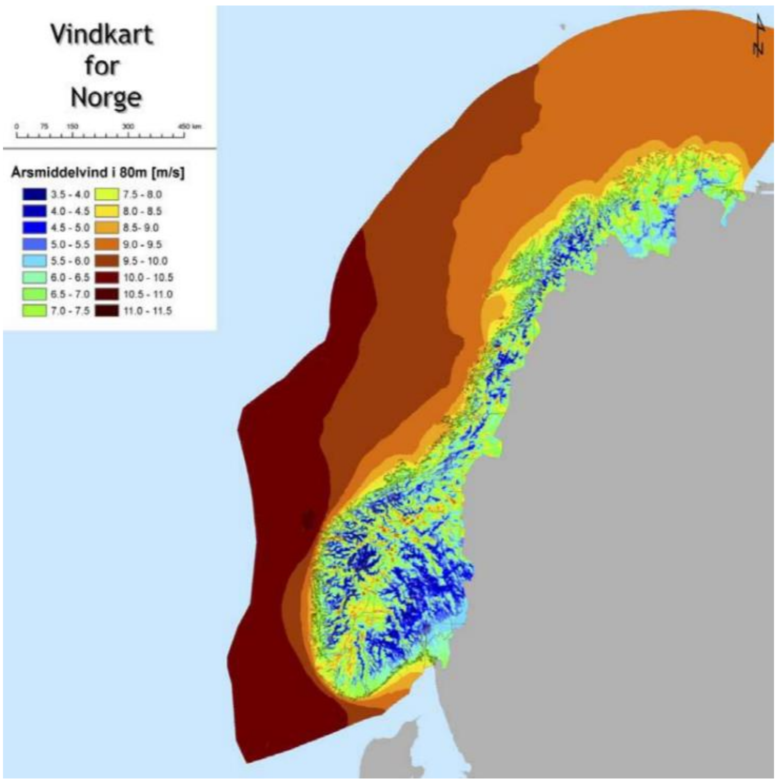

Figure 1 Wind speed potential at 80 m altitude

The success in development of possible future wind farms will rely on good estimates of weather conditions, regarding installation, operation and maintenance.
For this thesis, the goal is to compare weather data obtained from the ERA5 atmospheric reanalysis against local observational measurements at a given location offshore, and then investigate the effect of implementing the two sets of weather data in the simulation of a fictive windfarm.

The result from this thesis can potentially indicate the accuracy of using weather data from reanalysis datasets in future simulations for wind park development in the North Sea, and assess potential strengths and weaknesses in using reanalysis data in an offshore wind farm installation campaign.

2 Background

2.1 Climate reanalysis

Reanalysis datasets are widely used for monitoring climate change, for research and education and for commercial application. Forecast models and data assimilation systems are used together to reanalyse archived observations in the creation of large global datasets. These datasets can give valuable historic descriptions of the atmosphere, land surface and oceans.
A climate reanalysis typically contains atmospheric parameters such as rainfall, soil moisture, ocean wave height, sea surface temperature, wind speeds and more. By combining models and observations estimates are produced for locations all over the world and can span a time period of several decades (ECMWF, n.d-a).
Reanalysis creates large datasets, reaching size orders up to several petabytes. It is therefore advantageous to process the datasets via cloud-based tools, creating manageable download volumes.
Despite of reanalysis data having a hybrid origin, consisting of a combination of observations and forecast models, the data are often referred to as observations. It is though important to notice that reanalysis data should not be equated to real observations and measurements, due to some potentially significant differences.

The most important of these differences is argued to be that the errors and uncertainties associated with reanalysis are less well understood than the ones associated with the observations (Parker, 2016).

It is of great importance to be aware of the strengths and limitations of the reanalysis data for proper use and application.
ECMWF processes data from around 90 satellites as part of the data assimilation process (ECMWF, n.d-c). A total of 40 million observations are processed and used daily, with most of the observations originating from satellite data. ECMWF also includes other sources of available observations, such as ships and aircrafts, shown in Figure 2 (ECMWF, n.d-c).

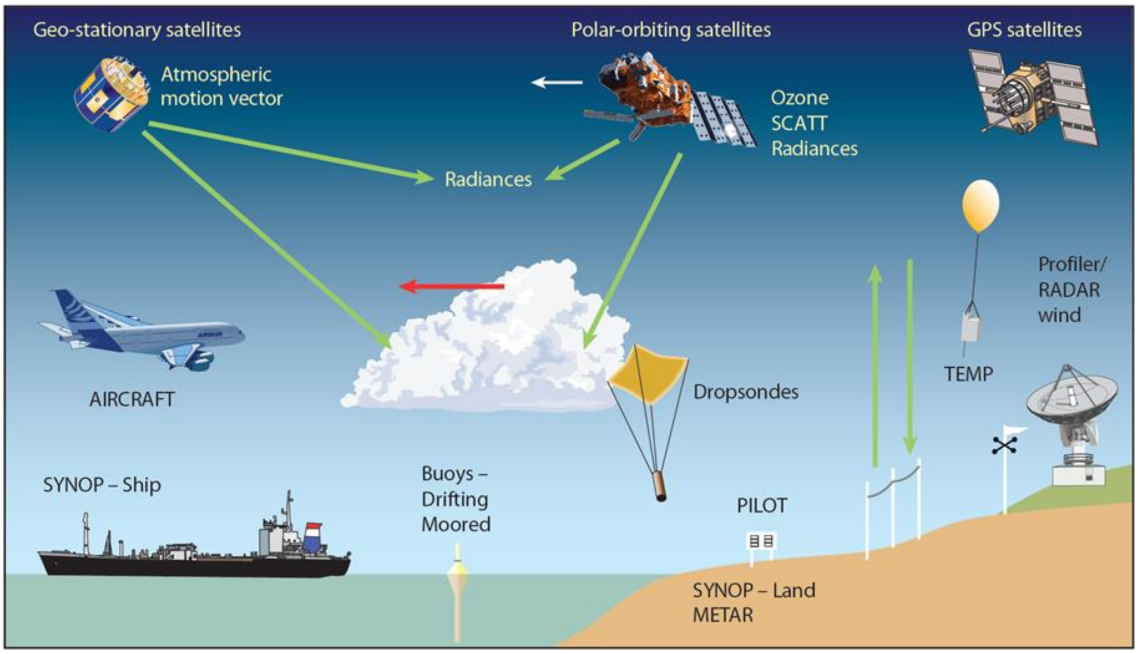

Figure 2 ECMWF observations

2.1.1 ERA5

The ERA5 reanalysis is the fifth generation of ECMWF atmospheric reanalysis of the global climate, replacing the previous ERA-Interim reanalysis which ECMWF stopped producing in August 2019 (Hersbach & Dee, n.d).
ERA5 is the first reanalysis produced as an operational service compared to the previous generations being research projects, and ECMWF is now contributing reanalysis data to the Copernicus Climate Change Service funded by the EU.

The completed dataset will when finished cover the period from 1950 until present. Per April 2020 historical data are available from 1979 until within 5 days of present. ERA5 also includes information about uncertainties for all values at reduced spatial and temporal resolutions (3-hourly intervals and a horizontal resolution of 62 km).

2.1.2 Ensemble forecasting

Weather observations are neither perfect nor complete, and since observational data cannot be collected at every single location of the desired resolution, some sort of approximation must be made. Also due to limitations in computational power, models inevitably approximate the equations for weather. This will cause uncertainties in the forecast produced.

The uncertainty will vary daily, dependent on the atmospheric conditions at the start of the forecast. Given atmospheric conditions such that the forecast is not very sensitive to the initial conditions, a forecast with a high degree of confidence can be produced. If though the atmospheric conditions cause a high degree of sensitivity in the initial conditions, the forecast produced will contain a higher degree of uncertainty from the beginning.

Ensemble forecasting is a method applied to address the uncertainties associated with forecasting and helps to predict the confidence in the forecast.

The system is called EPS has been operational at ECMWF since 1992 (ECMWF, 2012).

EPS represents the uncertainty by creating a set of 50 forecasts that start out with small variations in initial conditions of the atmosphere. These forecasts are based on the model that are close but not identical to the best estimate of the model equations, hence also addressing the uncertainties associated with the model on the forecast error. A control is also created, which represents the best estimate of initial conditions, giving a total of 51 integrations. Uncertainty of prediction can then be addressed by the spread of these 51 integrations at the given time.

The ensemble spread gives valuable information on the predictability of the atmospheric conditions and the range of uncertainty. Unpredictable atmospheric conditions will cause a stronger divergence in the ensemble members in the forecast.

Figure 3 illustrates the relationship between the spread of the ensemble members (yellow area), the ensemble mean, the control member and one of the ensemble members. The control member is not included as a part of the plume and can on some occasions be outside of the ensemble spread, on average 4% of the time (ECMWF, n.d-b).

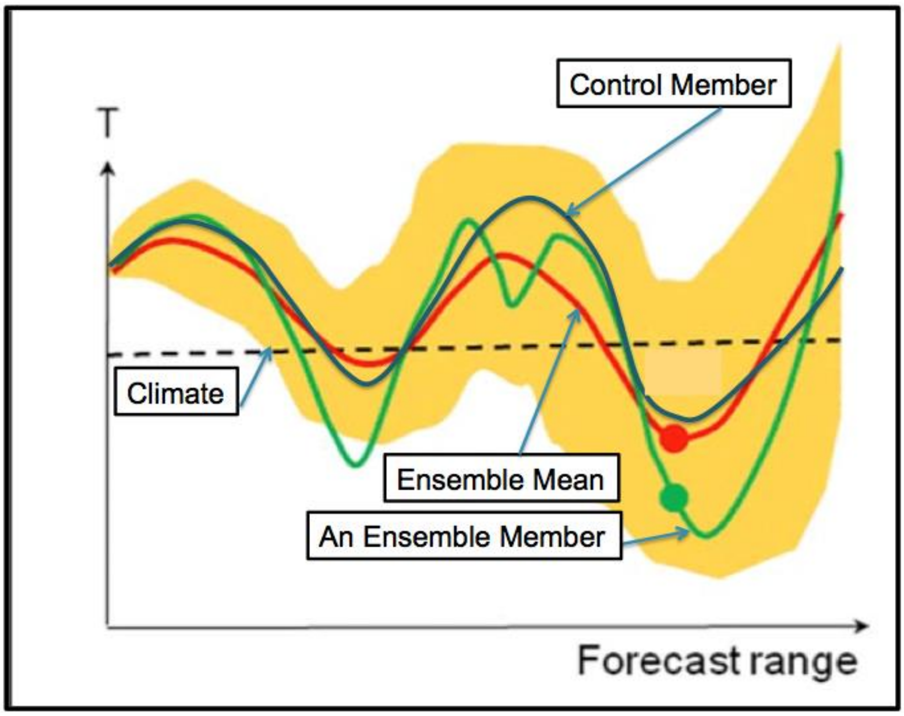

Figure 3 Ensemble forecasting

2.1.3 ERA5 Uncertainties

The uncertainties associated with the ERA5 reanalysis are available for all variables and can be accessed as the ensemble mean and ensemble spread.
Ensemble spread is the measure of the difference between the members, represented by standard deviation with respect to the ensemble mean.
By assuming a gaussian distribution of ensemble results, the ensemble mean should give an indication of variability (ECMWF, n.d-b).

Figure 4 shows the error on average for 850 hPa temperature for the Northern Hemisphere at various forecast-lead times, in addition to the ensemble spread.
The comparison of the root mean square error of the ensemble mean and the ensemble spread over lead time shows significant correlation. This indicates that that the spread is a good indicator of the likely error in the forecast.

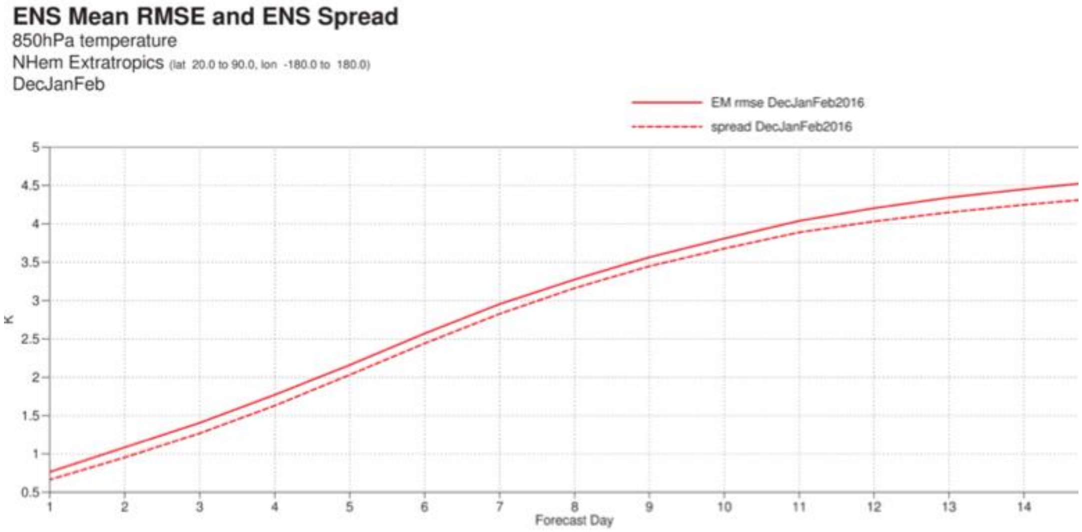

Figure 4 Correlation of ENS mean RMSE and ENS spread

2.2 FINO research platforms

In January 2002, the Federal Government of Germany decided the construction of three research platforms located in the North Sea and the Baltic Sea (FINO, n.d).
The locations for the three research platforms shown in Figure 5 were selected in suitable places in the vicinity of major offshore wind farms that were at the planning and application stage. Scientific studies conducted on these platforms include measurements of:

- Wind strength, wind direction and turbulence in relation to height
- Wave height and wave propagation
- Sea current strength
- Seabed surface conditions
- Lightning measurements

Ecological environmental research is also conducted such as monitoring bird strikes and benthic communities.

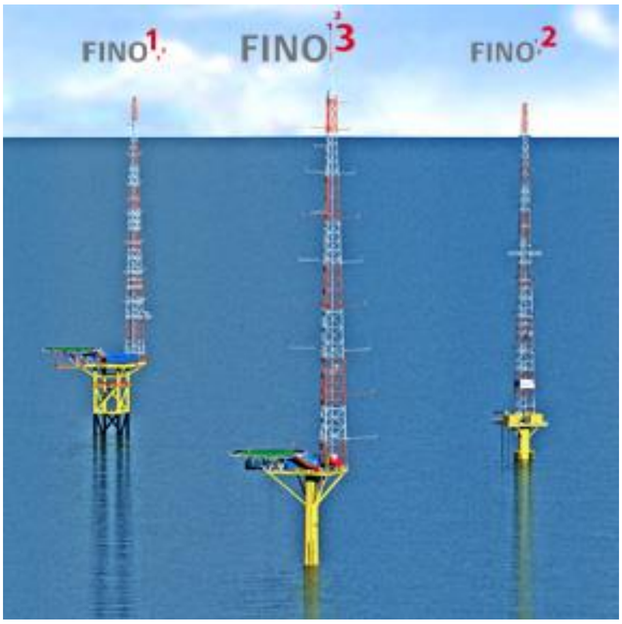

Figure 5 FINO research platforms

2.2.1 FINO3

The FINO3 research platform is located approximately 80 km to the west of Sylt, and measurements have been recorded under supervision of the Forschungs- und Entwicklungszentrum Fachhochschule Kiel GmbH since 2009.
FINO3 is located close to the operational wind farms Butendiek, DanTysk and Sandbank (FINO3, n.d-b).
The platform is equipped with a helicopter deck and a one ton lifting crane and is self-sufficient with electricity by three generators.
Total height of the structure is 172 meters, and a monopile foundation type is used with an anchoring depth of 30 meters at 22-meter water depth.
Observations are conducted between 30 and 100 meters.

2.3 Wind profile offshore

In the design process of a wind farm, it is of great importance to have a good estimate of the wind speed at specified heights.
When there is no measurement available at the altitude of interest, a wind profile is applied.
Due to factors such as roughness of the sea surface and atmospheric stability, different models can be applied.

In this study the Power Law is chosen for estimating the wind speed at hub height from the FINO3 observations.

$$U(z) = U_{hub} * (\frac{z}{z_{hub}})^{\alpha}$$

The Power Law outputs the average wind speed as a function of the reference height Z, where U_{hub} is the windspeed at height Z_{hub} and α being the power law exponent.
The power law is widely used in engineering due to its simplicity and creates a function with a close fit to the logarithmic wind profile.
Neutral stability is assumed with a constant roughness length of 0.002m to be used over the sea. The model does not take into account the roughness effects caused by waves or thermal effects due to atmospheric stability.
For use offshore, the IEC 641003 and GL standards recommend using a power law coefficient of $\alpha = 0.14$ (Obhrai, Kalvig, & Gudmestad, 2012).

2.4 Offshore wind farm installation

The installation process of offshore wind farms accounts for approximately 20-30% of the total development cost (M. Asgarpour, 2016).
Before the installation of the wind farm can take place, the components need to be designed, manufactured, and in most cases delivered to an onshore assembly site and assembled. The finished components can then be transported to the location of the offshore wind park and installation can begin.

2.4.1 Delivery of components and onshore assembly

Delivery of components to the onshore assembly site is the first step towards installation of an offshore wind farm. These components include the foundation, tower sections, nacelle and rotor. The onshore assembly site is the location where the component assemblies are completed and loaded onto transport vessels for transportation to the offshore wind park. Different assembly strategies exist, with the most common ones being:

I. No onshore assembly, all components are transported to the wind park location and then installed.
II. Tower assembly, the tower sections are assembled onshore for the complete tower to be transported and installed offshore.
III. Assembly of two blades and nacelle, where the nacelle, hub and two of the blades are connected before transport offshore.
IV. Assembly of three blades and nacelle, where the whole rotor is attached to the nacelle before transport.

Full assembly offshore has proven inefficient for larger wind farms and wind farms located far offshore. Tower assembly has proven great efficiency and today most wind farms are installed with preassembled towers. Onshore assembly of two blades and nacelle can be an efficient option if the transportation vessel has the proper deck configuration. The last strategy, assembly of all blades and nacelle onshore requires very specific transportation vessels and is rarely an optimal option.

The assembly concept must be chosen with respect to the wind farm location and size, as well as the availability of installation vessels. In most cases the tower assembly or the assembly of two blades and rotor will be most advantageous.

2.4.2 Offshore transport

The last step before final installation is the transport to the offshore wind park location. As mentioned in the previous chapter the wind turbine components are most often transported to the onshore assembly site for then to be loaded onto the transportation vessels, although in some cases the components can be shipped directly offshore.
Several types of vessels exist that are designed specifically for offshore wind turbine installation. The following types are most common for foundation, turbine and substation installation:

I. Floating vessel stabilized with mooring lines
II. Floating vessel equipped with motion-compensated crane
III. Jack-up barge

In general, the jack-up barges are mostly used for wind farms located close to shore, whereas the floating vessels with motion-compensated cranes are better suited for deep waters.
Specialized vessels are used for array and cable installation, customized for cable laying, trenching and rock dumping.
Sailing out to the location of the wind farm can only take place when the weather conditions are suited for the given installation step.
If not, the vessel will lay at harbour to wait for the proper conditions. The rate for the vessel still must be paid, and this term is called weather delay. This weather delay can constitute a large part of the project risk, especially for wind farms located far offshore.
Calculation of proper weather delay for all installation steps using historical weather data should be conducted, and the weather delay can be minimized by selecting the most ideal starting date for installation.

2.4.3 Offshore installation

Offshore installation is the process that start with the transportation vessel arriving with the foundations at the offshore wind farm site and end with cable installation vessels connecting export cables between the offshore substation to the onshore substation.
The installation process can be broken down into four steps:

I. Installation of foundation
II. Turbine installation
- Tower
- Nacelle
- Rotor

III. Installation of substation
  - Offshore substation
  - Onshore substation

IV. Cable installation
  - Array cables
  - Export cables

The installation strategy and selection of vessel will depend on the type of foundation for the wind turbine. Existing find farms today utilize bottom fixed foundation types, with the most common one being the monopile.
The monopile foundation reaches its engineering limits at about 30-meter water depth, and other bottom fixed structures such as jackets, gravity based, and tripods are used for depths up to about 60 meters (Myhr, Bjerkseter, Ågotnes, & Nygaard, 2014).
For exceeding water depths, floating turbines must be utilized.
It is estimated that up to 80% of the global wind power potential is located at depths over 80 meters, with the benefit of stronger and more consistent winds (Equinor, n.d).

Installation of foundation

The **monopile foundation** consist of a large hollow tube made of steel or concrete, with a diameter designed to match water depth, turbine size and soil condition. A layer of scour protection is added to the sea bottom, often in form of rock dumping at the monopile location. The monopile is then lifted from the transportation vessel and installed using eighter pile drilling or pile driving. On average this process takes about one to two days for the installation of each monopile. Due to the need for a stable platform for drilling or hammering, jack-up barges are commonly used.
After installing the monopile foundation a transition piece is necessary before the turbine can be mounted.

J**ackets and tripods** have similar installation processes, and like the monopiles they also need scour protection at the seabed. The jackets and tripods are then transported to the location using jack-up barges or floating vessels with mooring line stabilization, and then lifted and placed on the seabed. Piles in the foundation is then driven into the seabed for increased stability. The turbine tower can then be installed directly onto the topside of the jacket or tripod.

The **gravity-based foundation** requires seabed preparation to ensure flatness and scour protection. These foundation types are usually self-buoyant and are towed out to the wind farm location. After positioning the foundation is sunk by influx of water, and the foundation base is filled with ballast to anchor the foundation.

The turbine tower can then be installed.
Typical operational conditions for foundation installation is a windspeed below 12 m/s and wave height below 2m (Paterson, D'Amico, Thies, Kurt, & Harrison, 2018).

Turbine installation

After installation of the given foundation is completed, the turbine can be installed. The turbine can then be divided into four components, namely tower, nacelle, hub and blades. The first step is installing the tower, which is most often assembled at the onshore assembly site. In this case, the tower is transported offshore and lifted on top of the pre-installed foundation for then to be bolted in place.
For situations where tower components are not assembled at the onshore assembly site, they are transported directly to the wind farm location and assembled offshore. Assembly offshore is sensitive to weather conditions and is in most cases avoided if possible.
After tower installation is complete the nacelle is installed, lifted by a crane off the installation vessel and placed on top of the tower.
In cases where the blades are not pre-installed on the nacelle, they are lifted and mounted separately. It is common practice to keep the crane and vessel stationary and rotate the rotor for the installation of each of the blades.

Installation of sub-station

Offshore wind farms in the early 2000s were typically grid connected using 33kV alternating current (Higgins & Foley, 2014).
The wind farms then started moving further offshore and power generation increased, leading to the need for offshore sub-stations. An offshore sub-station will usually contain medium and high voltage transformers, switch gears, electrical generators, batteries and busbar systems for regulation of flow of electricity to the grid.
It has been shown that for distances over 90 km offshore, it will be cheaper to use high voltage direct current (HVDC) transformers instead of high voltage alternating current (HVAC) transformers for a 100 MW windfarm offshore (Bresesti, Kling, Hendriks, & Vailati, 2007).

For HVAC connection the export cables constitute the largest component cost, while for HVDC the substation itself is the most expensive component.
Though HVDC experiences loss in the transformer, the cable loss will be significantly lower for HVDC compared to HVAC. A comparative study found the following result for power loss as a function of cable length for HVAC vs HVDC transmission systems, assuming a power of 117 MW at 115 kV rated AC voltage (May, Yeap, & Ukil, 2016):

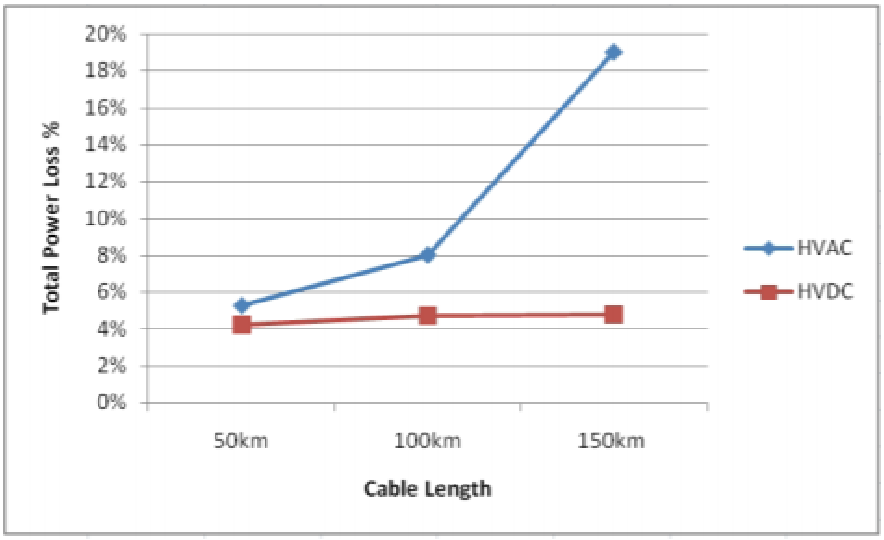

Figure 6 Power loss over cable length of HVAC and HVDC transmission

As seen in Figure 6, the power loss for HVDC would be significantly lower compared to HVAC for transmission over long distances.

Cable installation

The last step in the installation of an offshore windfarm is cable installation. The array cables connect the individual turbines to the substation or substations.
The electricity is then transported through the export cables to the onshore substation before being coupled to the local electrical grid.
Array cables and export cables are planned in such a way that the cable length is minimized to save money and reduce current loss.
For the cable laying vessels, the weather criteria for operation is typically limited to a wave height of 1,5 m and wind speed of 15 m/s for cable installation, and 3 m wave height and 12 m/s wind for cable burial (Paterson et al., 2018).

Both array cables and export cables are buried in the seabed using trenching ROVs. Different approaches for burial depths exist and are often divided into risk or prescriptive based approaches. Germany uses the prescriptive based approach, having decided that wind farm export cables and interconnections in the North Sea require a burial depth of minimum 1,5 meter (DNV-RP-J301).

2.4.4 Installation strategies

In the planning phase of an offshore wind farm, it is desirable to choose a location that offers a high wind power potential. These locations are likely to produce both large wind speeds and wave heights, affecting the installation process by narrowing the time window for safe installation (Vis & Ursavas, 2016).
Two different procedures were formerly used due to the uncertainty of the weather and the weather forecast. In the summer, a single task could start when it could be accomplished within a good weather forecast, for example a one component lifting operation.
In the winter, a cycle from loading, shipment, installation and return to port would only start if the weather forecast were good for the complete cycle.
Increased quality of weather forecasting has led to the winter procedure being less commonly used.
(Vis and Ursaves, 2016) state that the major factors in the logistics of an offshore wind farm installation is pre-assembly, vessel load and distance to shore.

They suggest a pre-assembly strategy comprised of a minimum number of components for onsite installation and a maximum number of turbines for loading on a vessel, and state that the findings are especially important for installation of new wind farms located further offshore.
(Masoud Asgarpour, Dewan, & Savenije, 2014) state that future wind parks will be located further offshore in deeper water and harsher weather conditions, and that the installation process of an offshore wind farm is influenced significantly by weather conditions. The installation costs are stated to be dominated by vessel and equipment hiring cost.
Installation practices for reduction of these costs include:

- The use of larger and faster installation vessels. Potentially offshore transfer of components from support vessel to jack-up installation vessels, avoiding the need for these high cost vessels spending time on transportation to and from port.
- Complete pre-assembly of turbines onshore, for one-operation installation of the turbine and foundation.
- Use of multiple harbours for reduction of transportation cost of arranging components, and transportation time from nearest harbour to wind farm location.
- A more holistic consideration in cable design and installation requirements due to the large number of cable damage incidents and cost overruns related to subsea cables.

3 Data description

3.1 FINO 3 data

The 120-meter tall FINO3 offshore measurement platform has instruments located at eight heights between 30 and 100 meters, and measurements of wind speed and wind directions are carried out using wind vanes and anemometers.
Several other meteorological measurements are also observed, including air temperature, moisture, air pressure, global radiation, relative humidity and precipitation.
The distribution of measuring instruments located on the FINO3 mast is shown in Figure 7 (FINO3, n.d-a).
Oceanographic data are measured using a wave buoy, obtaining information on wave height, wave period and wave direction.

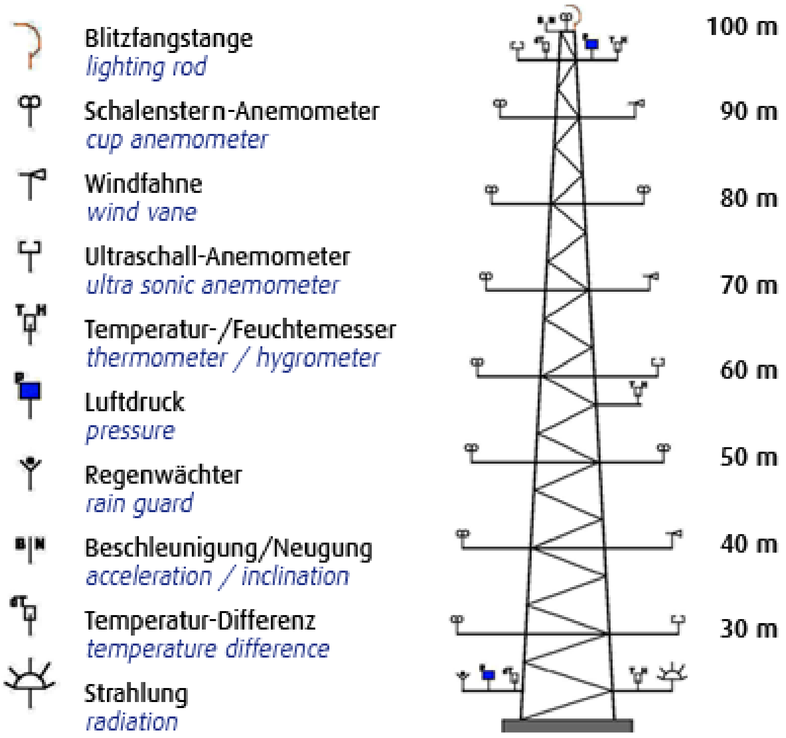

Figure 7 FINO3 measuring instruments

A total of seven years of observational data from FINO3 was obtained after access was granted to the FINO databank, in the period 2013 to 2019. These data contained information on wind speed and direction, as well as wave amplitude.

3.1.1 Data processing

To minimize the effect of mast distortion, the FINO3 platform is designed with a triangular cross-section with up to three booms on each of its eight measurement heights, shown in Figure 8.

It is desirable to avoid measurements from sensors that are significantly affected by the wake created by the mast. The actual windspeed is therefore decided by first considering the wind direction, and then selecting wind speed measurements from booms in the wind sectors undisturbed by the mast. Dividing into sections A, B and C at respectively 225º, 345º and 105º allows further selection of wind sectors that are undisturbed.

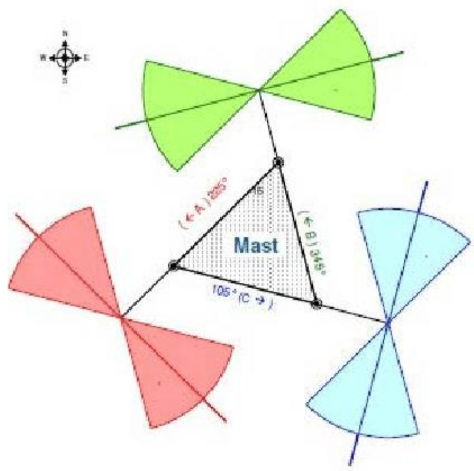

Figure 8 Orientation of the booms on FINO3, with corresponding undisturbed sectors.

Possible wind directions were then divided into six sectors as shown in Figure 9 (Obhrai et al., 2012). It is then assumed that wind speed measurements are undisturbed by the mast in the following sectors for boom A, B and C respectfully, presented in Table 1:

Table 1 Sectors unaffected by wake for boom A, B and C.

Boom	Unaffected sector 1	Unaffected sector 2
A	105° to 165°	285° to 345°
B	45° to 105°	225° to 285°
C	165° to 225°	345° to 45°

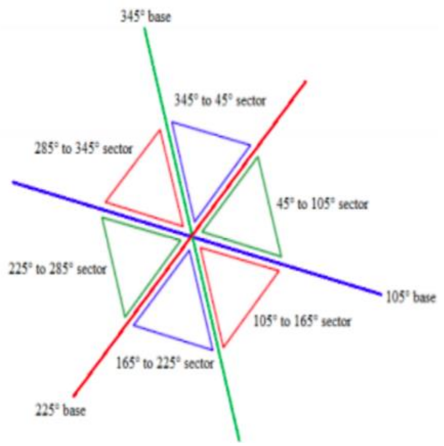

Figure 9 Six sections of wind at FINO3

The wind data obtained from the FINO databank was downloaded in the form of three .dat-files, one file for each of the booms at the specified height. A code was then created in the MATLAB software to obtain a continuous wind speed time series.

The highest elevation containing wind data from all three booms is located at 92 meters, and this altitude was chosen for further study.

The wind data measurements are stored in 10-minute intervals, and wave data every minute.

Since the timestep in the ERA5 reanalysis is one hour, every sixth value of the wind data was chosen and every sixtieth value of the wave measurements, to end up with hourly observational data.
Un-available data was identified as large negative values in the dataset for both wind speed and wave amplitude (-999), these measurements were set to non-numeric for future comparison with the ERA5 time-series.
For proper comparison with the ERA5 dataset at hub height altitude, the wind data had to be corrected from 92 meters to 100 meters. This correction was done using the Power Law described in chapter 2.3.

3.2 ERA5 data

The full ERA5 reanalysis dataset has a size of about 9 Petabytes, covering the Earth with a grid resolution of 0,28215º for atmospheric data and 0,36 º for wave data.
Due to its large size, the CDS dataset can be accessed eighter via a web interface or programmatically using the CDS API service.
A code was created in the CDS toolbox to access the data needed (Included in Appendix).
The code was created to access the desired outputs from ERA5 for the given years, months, days and hours specified.
Data retrieval time was drastically improved when adding an "area"-input, specifying a range for latitude and longitude to retrieve data from. A function to extract the data from only a specified point was added, in addition to a function creating a download file of the output data.

3.2.1 Data processing

The output datafiles were downloaded in a NetCDF file-format, and then read and converted into numeric matrices using MATLAB software.
The windspeed data was expressed as zonal and meridional components, with a positive u-component meaning wind blowing in eastward direction and a positive v-component meaning wind blowing to the North (EOL, n.d).

It is important to be aware of the different ways of referring wind directions since these wind directions blowing towards East and North are often referred to as “westerly” and “southerly” winds. In addition, it is common practice to describe the wave direction as the direction the waves are coming from.

The wind speed was determined taking the square root of the sum of the squared u and v-components:

$$U = \sqrt{u^2 + v^2}$$

The wind direction was established taking the arctangent of u-component of the wind divided by the v-component.

All the non-numeric values in the FINO3 time series measurements had to be identified, for then to find the matching timestamp in the ERA5 dataset and set the corresponding value as non-numeric.

A continuous dataset was made by removing the non-numeric values, to be able to import the weather data into the Shoreline wind park simulation tool.

3.2.2 ERA5 observations in area of investigation

The models used in the ERA5 reanalysis use weather observations for correction and increased accuracy. Therefore, the accuracy of the forecast will depend on the availability of weather observations in the area of interest.

A search was performed on request by the observation expert in the Copernicus scientific team. The search aimed to locate all recent wind observations made for the ERA5 reanalysis within specified coordinates, and yielded a list with the parameters specified in Table 2:

Table 2 ERA5 observations at FINO3 location

Lat	**Lon**	**Start date and hour**	**End date and hour**
54-56	7-9	January 1, 2019 00:00	April 30, 2020 23:00

A total of close to 11 000 measurements of the 10-meter wind speed were logged within the specified time period and coordinates. The data originate from ship reports and accounts for all observations for this area except for aircraft reports. The list was loaded into MATLAB and the location of the measurements was plotted. Figure 10 shows the locations for ERA5 observations in addition to the location of FINO3.

These observations in addition to aircraft and satellite data are used in combination with different models for creation of the reanalysis.

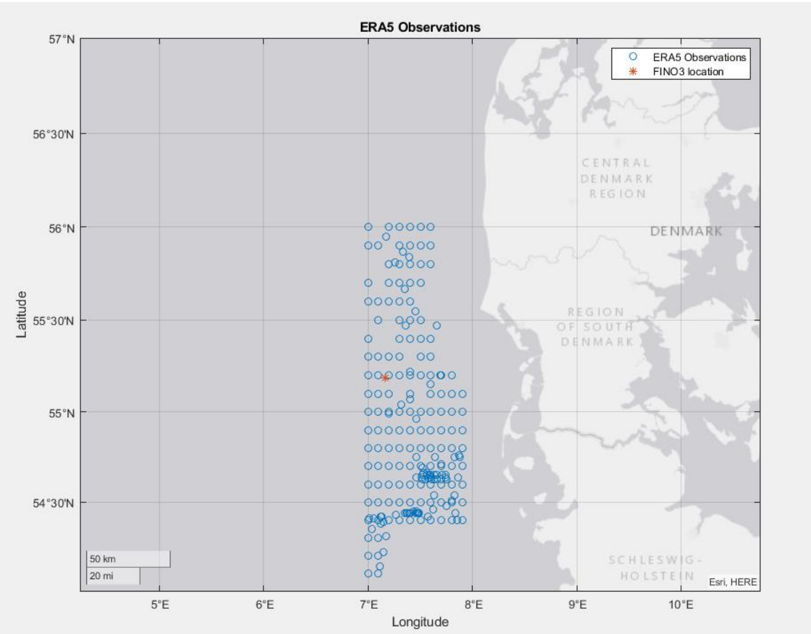

Figure 10 ERA5 Observations at FINO3 location

Other methods that are not directly included in the reanalysis can still serve as additional validation of the forecast in areas of open sea.

Radar-Altimeter 2 (RA-2) is an instrument on the ENVISAT satellite that transmit radar pulses towards Earth (Abdalla, Isaksen, Janssen, & Wedi, 2013).

The strength of the backscatter of the signal is inversely proportional to the ocean roughness. Furthermore, the sea surface roughness is shown to be closely related to the surface wind speed.

Though RA-2 is not part of the Integrated Forecast System but rather used for independent validation, Abdalla et al. states that RA-2 surface wind speed measurements can be an attractive source of data to study the properties of the atmospheric spectra at the ocean surface.

3.3 Assumptions and approximations

For proper comparison, the wind observational data from FINO3 must be corrected from 92 meters to 100 meters.
This correction was made using the Power Law with a coefficient of $\alpha = 0.14$. This model does not take into consideration the roughness of the ocean surface nor the thermal effects due to atmospheric stability.
It is though reasonable to believe that the correction from 92 meters to 100 meters will result in a relatively small increase in wind speed.
The mean value of wind speed from FINO3 after correction from 92 meters to 100 meters using the Power Law, increased from 9,6264 m/s to 9,7395 m/s. This represents an increase in windspeed of approximately 1,17 %.

To be able to conduct a simulation of a wind farm installation using the Shoreline simulation tool, a continuous dataset is needed. This means removal of the non-numeric values from gaps in the observational data from FINO3, and the corresponding timestamp for ERA5. Figure 11 shows the continuous dataset from ERA5 wave height plotted over time. The largest single gaps are found between May-September 2016 and April-June 2019, and a total of 409 days are lost creating this continuous dataset, representing 18,7% of the dataset.

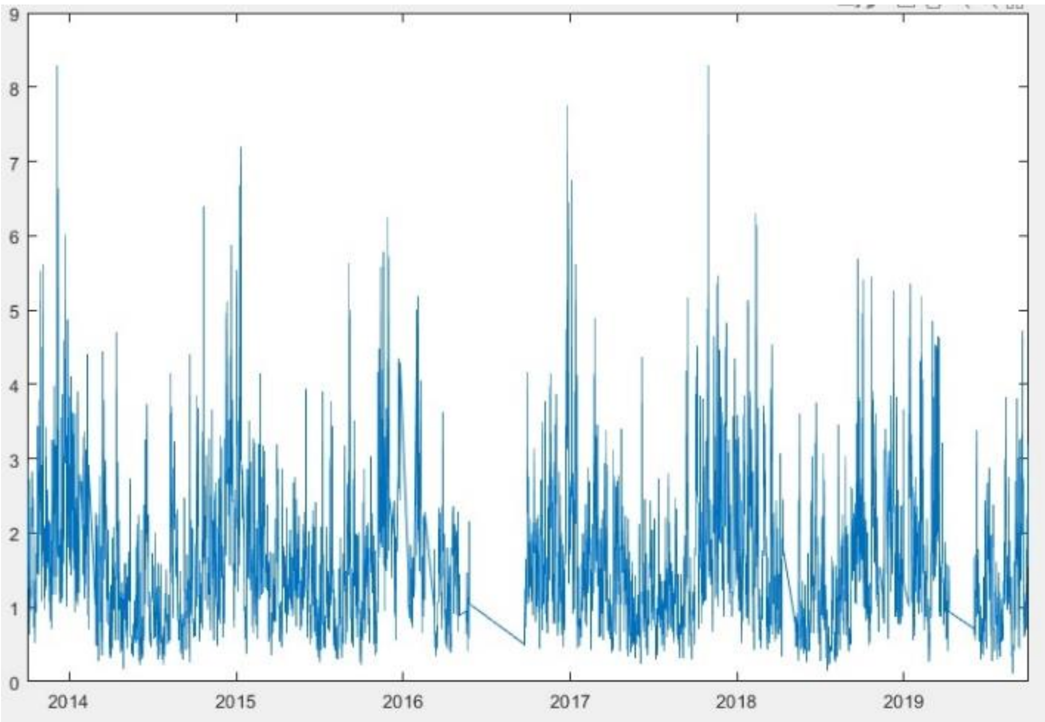

Figure 11 Continuous wave data from ERA5

4 Comparison of datasets from ERA5 and FINO3

After accessing and processing the data from FINO3 and the ERA5 reanalysis as described in chapter 3, a matching time series containing hourly measured wind and wave data was obtained for the period 01.10.2013 00:00 to 30.09.2019 23:00.

This adds up to a total of 52584 timestamps, containing sections of unavailable data for the wind speed and wave height dataset.

4.1 Wind speed time series comparison

After filtering of bad data (data of value -999 due to technical error, maintenance or general downtime) the dataset for further comparison consisted of 42763 recordings.

MATLAB was then used for further analysis to obtain the parameters shown in Table 3.

Table 3 ERA5 and FINO3 100-meter wind speed dataset comparison

Dataset	Mean wind speed	Correlation coefficient	Standard deviation	Variance	Root mean square error
FINO3	9,657 m/s	0,943	1,029 m/s	1,058 m/s	1,544 m/s
ERA5	9,804 m/s				

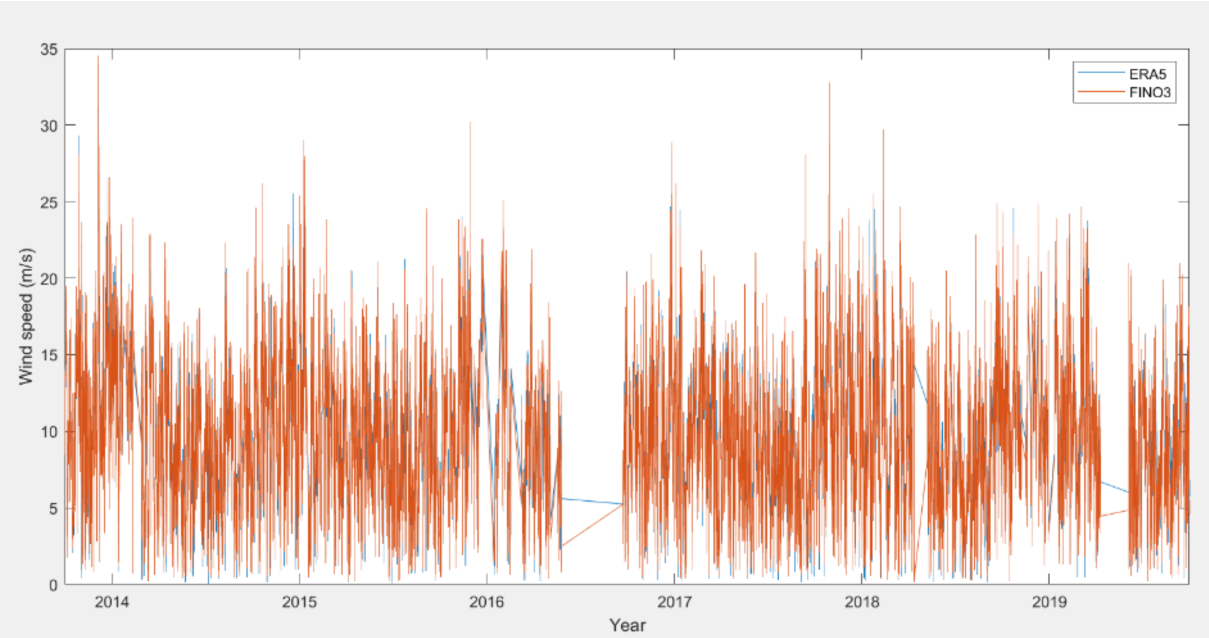

Figure 12 ERA5 and FINO3 wind speed plot

Figure 12 shows the wind speed at 100-meter altitude from the ERA5 reanalysis and FINO3 observational metrological mast plotted together. The spread between the data was found by subtracting the values of the FINO3 dataset from the ERA5 dataset and plotted in Figure 13. Negative values on the graph refers to FINO3 wind speeds larger than from ERA5.

84,1 % of the data lies within a wind speed spread of 2 m/s, and 94,9 % within 3 m/s spread.

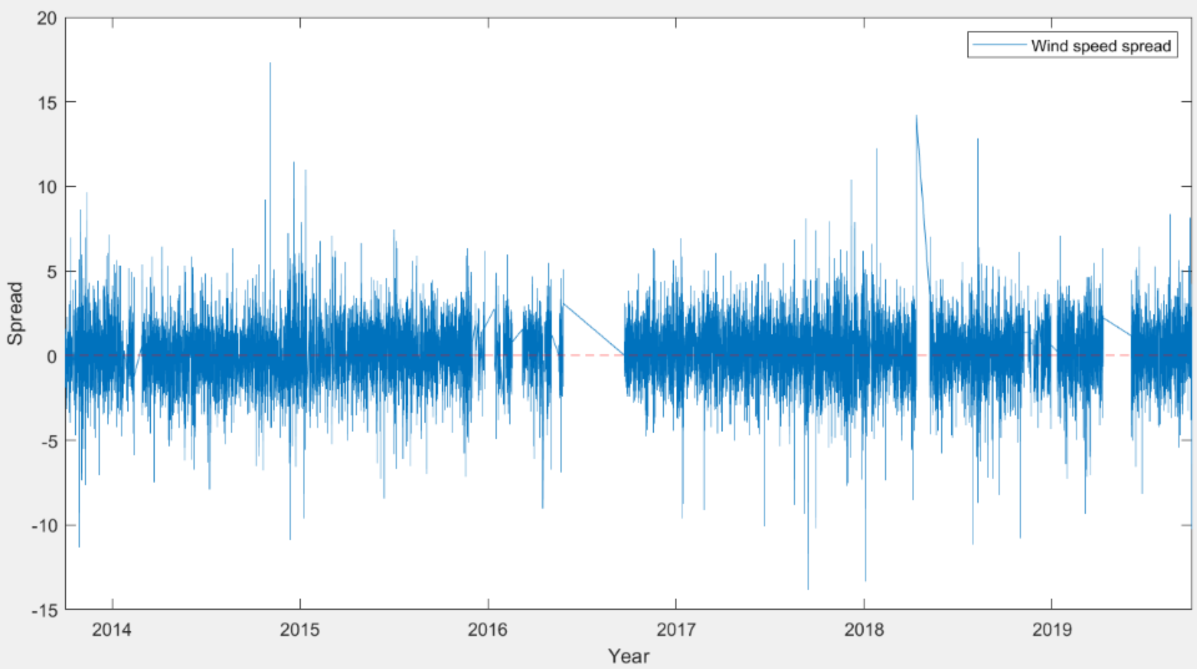

Figure 13 Wind speed spread plot

In Table 4 the amount of data over a given wind speed limit is given. The ERA5 reanalysis has an overall higher estimate of wind speed, though the FINO3 measurements contain slightly more high wind speed observations, as can be seen by the peaks on the graph in Figure 12.

A search was performed to find the number of wind speed values over 23 m/s for both datasets, resulting in 245 values for the FINO3 dataset and 174 for the ERA5 dataset.

Table 4 Percentage of data over given wind speed for FINO3 and ERA5 datasets

Dataset	**Wind speed>4 m/s**	**Wind speed>8 m/s**	**Wind speed>12 m/s**	**Wind speed>16 m/s**
FINO3	89,41 %	60,81 %	29,26 %	9,32 %
ERA5	90,52 %	63,63 %	30,32 %	8,69 %

4.2 Wave height comparison

The wave data was filtered in the same way as the wind speed data, by locating the invalid or missing data in the FINO3 observational measurements and defining the respective data value and corresponding value in the ERA5 dataset as non-numerical.

The data was then analysed to obtain the values given in Table 5.

Table 5 ERA5 and FINO3 wave height dataset comparison

Dataset	Mean wave height	Correlation coefficient	Standard deviation	Variance	Root mean square error
FINO3	1,602 m	0,955	0,223 m	0,050 m	0,283 m
ERA5	1,565 m				

The seasonal variations in wave height are clearly shown for both datasets when plotted in Figure 14, with higher average and peak values for wave height occurring in the fall to winter months.

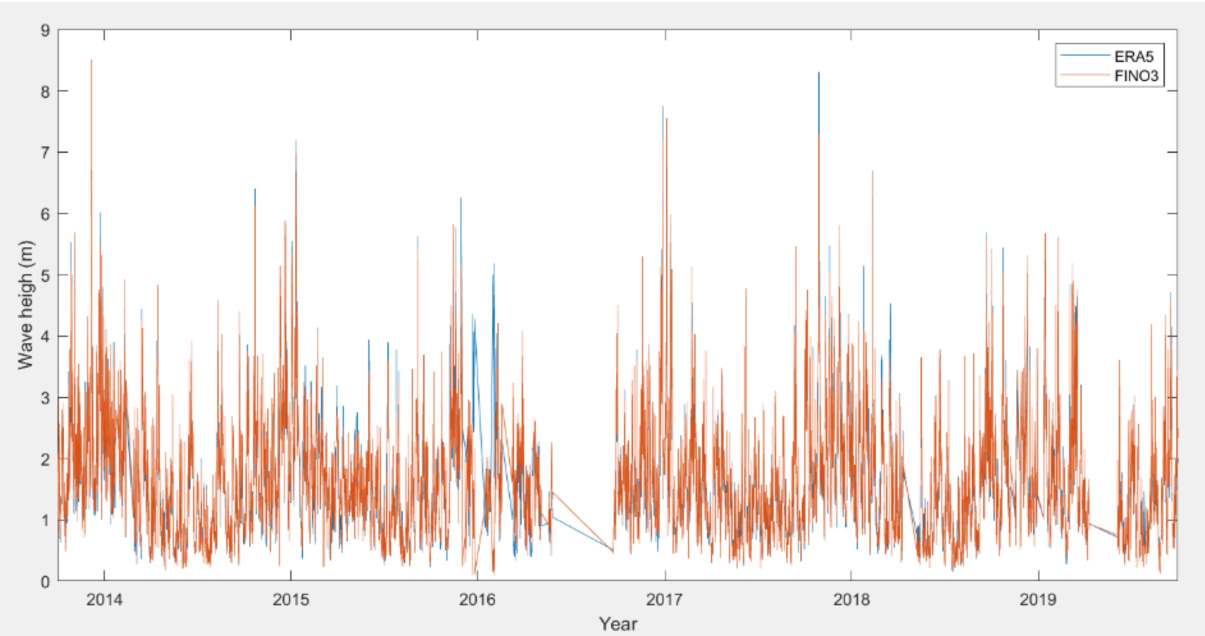

Figure 14 ERA5 and FINO3 wave height plot

In Table 6 the amount of data over a given wave height limit is given. It shows that the FINO3 dataset contains more data elements in the area 1-2-meter wave height compared to ERA5. This is also reflected in the higher average value of the FINO3 wave height dataset.

Table 6 Percentage of data over given wave height for FINO3 and ERA5 datasets

Dataset	Wave height>0.5m	Wave height>1m	Wave height>2m	Wave height>3m
FINO3	93,66 %	71,21 %	27,47 %	7,67 %
ERA5	93,86 %	68,59 %	25,20 %	8,11 %

The wave height spread was found by subtracting the value of the FINO3 data from the ERA5 data and plotted as shown in Figure 15. Negative values refer to FINO3 wave heights greater than corresponding estimate from ERA5.

95,6 % of the data is within a wave height spread of 0,5 meters, and 78,9 % within a spread of 0,25 meters.

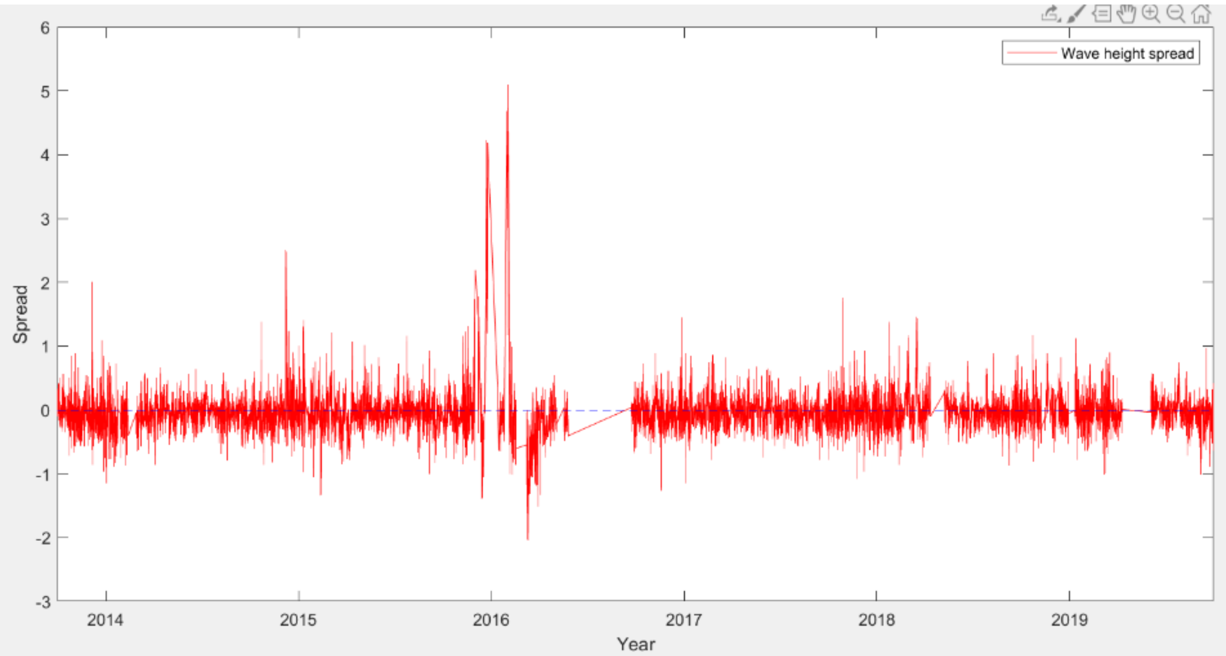

Figure 15 Wave height spread plot

4.3 ERA5 dataset uncertainty assessment

As mentioned in chapter 2.1.3 the ERA5 reanalysis dataset includes information on uncertainties in the forecast in form of ensemble spread and ensemble mean. The ensemble spread is a measure of the difference between the members in the ensemble with respect to the ensemble mean and is offered in three-hour intervals unlike the forecast data provided hourly.

The ensemble spread data was obtained for the 100-meter u and v component of the wind speed. The RMS value of the u and v component was found to obtain the ensemble spread for the wind speed.

Figure 16 shows the ensemble spread values of the 100-meter windspeed in the ERA5 reanalysis, for the time period considered in this study. The mean value of the wind speed spread is 0,494 m/s.

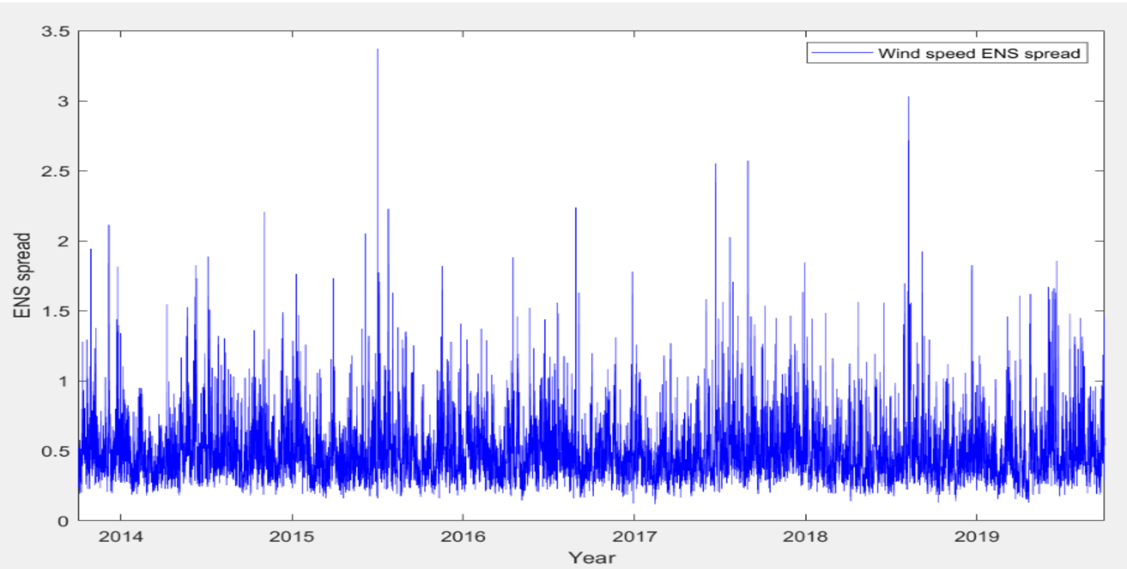

Figure 16 ENS spread of wind speed data from ERA5

Ensemble spread for ERA5 wave height was obtained and plotted in Figure 17. The mean of the ENS spread was found to be 0,030 m.

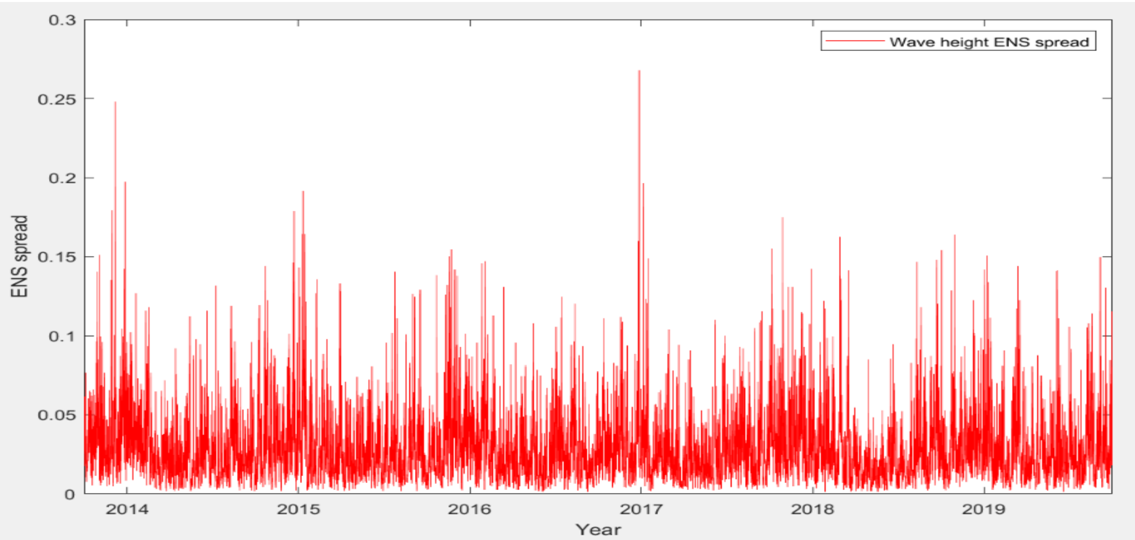

Figure 17 ENS spread of wave height data from ERA5

A comparison was also made between the ensemble mean of the ERA5 reanalysis and the forecast data for wind speed. The data value of every third hour was extracted from the hourly forecast and plotted against the ENS mean.

These datasets were expected to have a strong correlation, though a difference because a strength evaluation on the initial conditions is also a factor in the final forecast (Toth & Buizza, 2019).

Figure 18 shows the ensemble mean plotted against the forecast data for wind speed. The data correlation factor is 0,978 and a standard deviation of 0,673 m/s was found.

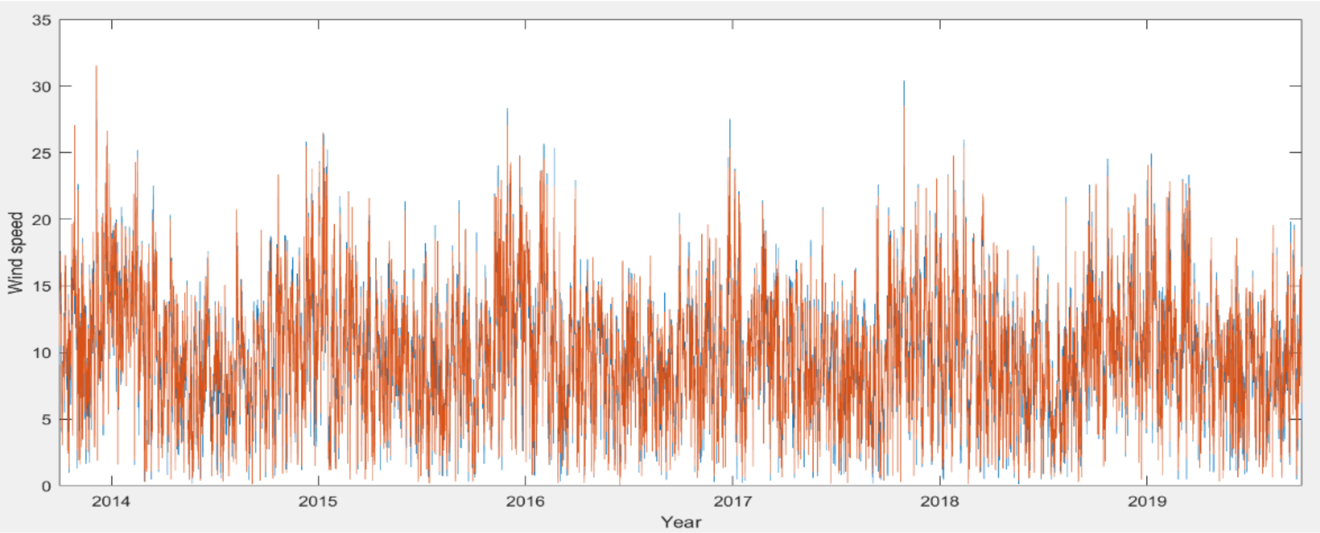

Figure 18 ERA5 Wind speed forecast vs ENS mean

5 Simulation of wind park installation campaign

The wind and wave data from ERA5 reanalysis and FINO3 observations was loaded into SIMSTALL, an intelligent simulation tool from Shoreline to assess the installation time and the accumulated waiting on weather (AWoW) in the installation of a fictive wind farm.
A base case that represents a typical offshore wind farm was created to be able to simulate a wind farm installation. For this study, the layout and location of NORCOWE reference wind farm was chosen (Bak & Graham, 2015).
The simulation was then performed for different starting months, to investigate the sensitivity of AWoW to installation start month.

5.1 Base case description

A base case was created for simulation purposes consisting of 80 wind turbines with 10 MW rated power. The DTU 10-MW reference turbine was selected, with specifications listed in Table 11 in Appendix (Luo, Tian, Wang, & Liao, 2018). The turbines are placed on monopile foundations and assumed to have a hub height of 108 meters. Like the NORCOWE reference wind farm, the base case is also located at the location of the FINO3 met mast.

A Curvilinear turbine layout was chosen, identical to the layout of the NORCOWE wind farm (Frøysa, 2016). Figure 19 shows the turbine layout exported from the Shoreline simulation tool:

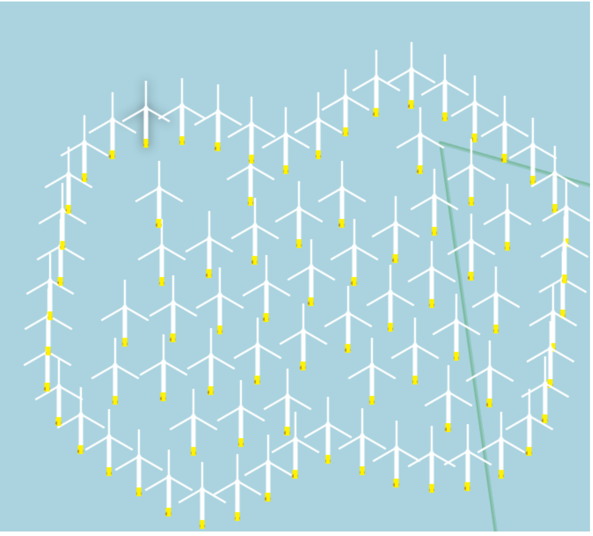

Figure 19 Base case turbine layout

5.2 Simulation of installation campaign

As earlier described in section 2.4, the operations of a wind farm installation consist of installation of foundations, turbines, substations and cables. For the installation campaign in this study the installation of foundations and turbines will be considered.
The different components are assumed delivered to the harbour and available for loadout at any time. The components are then loaded onto the turbine installation vessel (WTIV), capacity and limitations of the vessel used in this study are shown in Appendix, Table 10. Different activities by the WTIV are constrained by wave height and wind speed for safety reasons. The vessel will travel to installation site when fully loaded and the weather is within specified criteria. Before lifting operations offshore, the WTIV must be jacked up.

This process is also restricted by weather conditions. After installation of the components the ship returns to port for reloading.
In the base case of this study the monopile foundations are installed by pile driving, and the installation of transition pieces will start first when all foundations are installed. After completed installation of foundations and transition pieces the turbines are installed. The wind turbine components are assumed preassembled in 5 parts: complete tower, nacelle with hub and the three blades.

Tower is installed first, then the nacelle, and finally the three individual blades are attached to the hub which was preassembled to the nacelle.
Wave height and wind speed were used as limiting criteria for the operations during simulation of the installation campaign. Operation duration for each operation are given in Appendix, Table 12 from the Shoreline simulation tool. Required weather window duration is set to twice the operation duration, as suggested in DVV-OS H101.

5.3 Wind and wave weather window analysis

As wind farms are developed on challenging locations further offshore, the weather in these areas becomes more unpredictable. Safe and efficient operations have a great dependency on weather factors such as wind speed, wave height and current. For weather sensitive operations it is especially important to have knowledge about the probability of experiencing acceptable weather conditions and the corresponding waiting time. In cases where the probability of experiencing these acceptable weather windows are too small and the expected waiting time too long the operation schedule may be reviewed to eighter alter the design or selection of installation equipment enabling installation in more severe weather conditions, or alter the schedule to a period with better chance of experiencing good weather windows (Chen & Mukerji, 2008).

5.3.1 Wind weather windows

After dividing the operations in the base case into operational categories based on maximum wind speed limit and the installation duration, the wind weather windows were established (Beinke, Ait Alla, & Freitag, 2017). Information about the different operation categories a-l is shown in Table 7.

MATLAB was then used to find the number of available wind weather windows for the different categories in the wind data from ERA5 and FINO3.

Table 7 Wind weather windows for installation campaign

Weather window (Hours)	Wind speed limit (m/s)	Reference height (m)	Installation operations	Number of wind weather windows
5	12	92	A • Loading of blade set	FINO3: 4393 ERA5: 4590
3	14	92	B • Loading of tower	FINO3: 8262 ERA5: 8622
4	14	92	C • Loading of transition piece • Loading of nacelle	FINO3: 6566 ERA5: 6859
4	18	92	D • Loading of pile	FINO3: 7952 ERA5: 8093
4	8	108	E • Installation of each blade	FINO3: 2495 ERA5: 2546
6	10	108	F • Installation of nacelle	FINO3: 2594 ERA5: 2703
2	12	108	G • Positioning during jack up • Preparation of transition piece for tower installation Preparation for lifting during generator installation	FINO3: 8937 ERA5: 9248
8	12	108	H • Tower installation • Securing generator	FINO3: 2702 ERA5: 2850
2	18	108	I • Monopile stabbing	FINO3: 13214 ERA5: 13443
4	18	108	J • Monopile upending from vessel	FINO3: 7864 ERA5: 8015
6	18	108	K • Piling • Installation of transition piece	FINO3: 5576 ERA5: 5686
12	18	108	L • Airtight Platform and bolting	FINO3: 2940 ERA5: 3023

As can be seen in Figure 20 the number of available windows decreases as the duration of the operation increases, and the number of windows decreases as the maximum allowed windspeed decreases.

Operation "e" referring to the installation of the turbine blades had the lowest number of available windows and is dominated by sensitivity for maximum wind speed.

Operation "I" had the largest number of available operation windows, referring to stabbing of the monopiles. This operation has a low duration of only 2 hours and a high wind speed limit of 18 m/s.

It was found that the number of available wind weather windows are slightly higher for the wind data from ERA5 compared to data from FINO3.

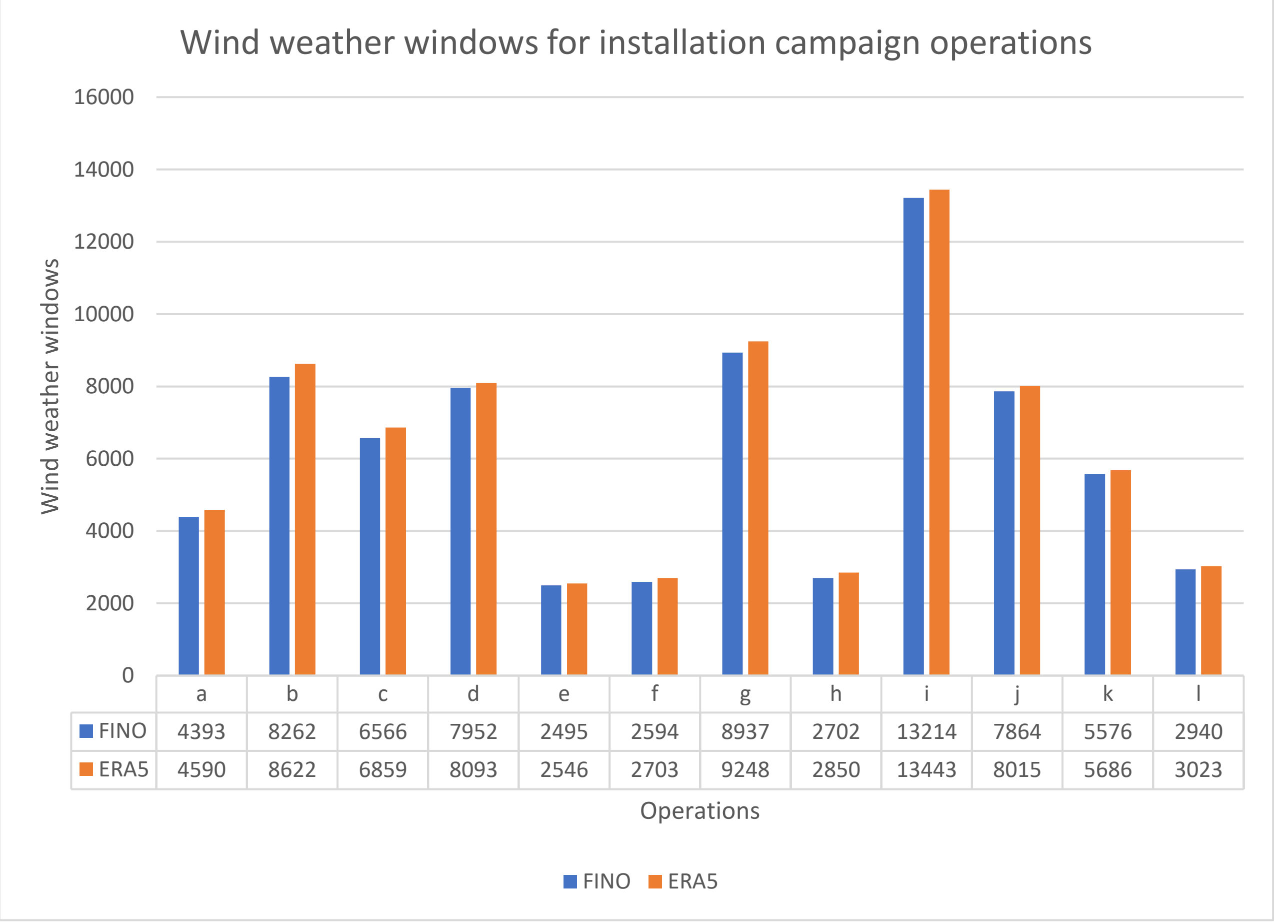

Figure 20 Number of wind weather windows for installation campaign operations

The fact that the ERA5 wind speed data has a higher mean value than observational data from FINO3 but still more wind windows could possibly indicate that the data from ERA5 are more smoothed out, containing fewer single values to exceed a potential weather window.

5.3.2 Wave weather widows

The installation vessel used in the base case (WTIV) has a wave height limit of 2,8 meters for transit to and from the wind farm, and 1,5 meters for the jack-up.
For installation of the turbine foundation, the wave height is limited to 3 meters, and as mentioned in chapter 2.4.3 the typical limit for cable installation and burial is 1,5 meters and 3 meters respectfully.
The wave weather window analysis is therefore conducted for a wave height of 1,5 meters and 3 meters, and a time series of 2-10 hours.
Table 8 shows the resulting number of available wave weather windows for both ERA5 and FINO3.

Table 8 Wave weather windows for installation campaign

Window time (h)	Wave height limit (m)	Number of wave weather windows
2	1,5	FINO3: 7040 ERA5: 7819
	3	FINO3: 12888 ERA5: 12950
4	1,5	FINO3: 4093 ERA5: 4586
	3	FINO3: 7681 ERA5: 7717
6	1,5	FINO3: 2853 ERA5: 3215
	3	FINO3: 5447 ERA5: 5496
8	1,5	FINO3: 2178 ERA5: 2454
	3	FINO3: 4209 ERA5: 4251
10	1,5	FINO3: 1736 ERA5: 1974
	3	FINO3: 3425 ERA5: 3452

The available wave weather windows for 1,5-meter wave height in the FINO3 and ERA5 datasets are showed in Figure 21.

As shown in chapter 4.2, a higher mean value for wave height was found in the FINO3 dataset compared to the ERA5 dataset.

This is reflected in the available wave weather windows with a higher number of windows available in the ERA5 data.

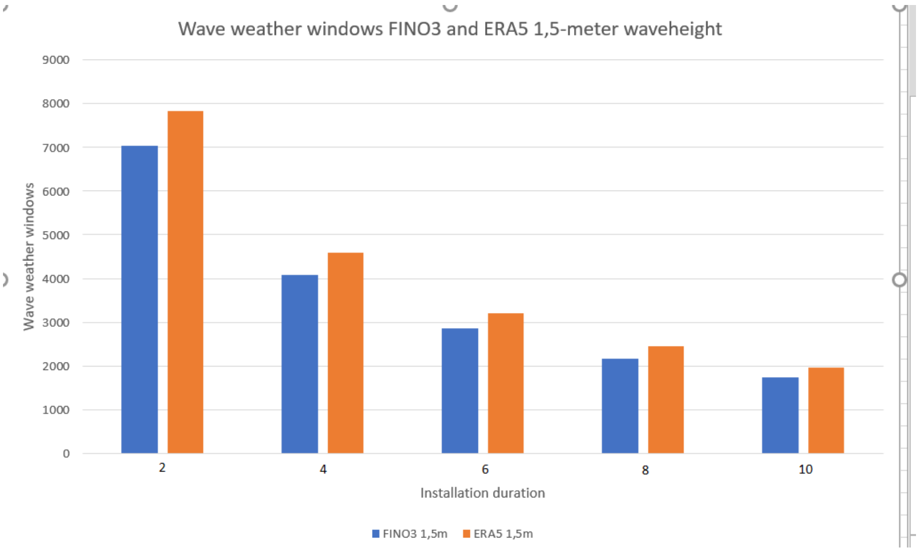

Figure 21 Wave weather windows for FINO3 and ERA5, 1,5-meter wave height

5.4 Accumulated waiting on weather

The simulation was carried out based on the complete installation of 80 turbines, using the wind and wave weather data from FINO3 and ERA5 respectfully.

Difference in the weather data will affect the time to complete the installation and the accumulated waiting on weather.

The installation campaign of the base case described in chapter 5.1, consisting of the installation of 80 monopiles, transition pieces and turbines, was simulated in Shoreline. Time for completion of the installation process when not including any weather restrictions was found to be 311 days.

5.4.1 Accumulated waiting on weather for different starting months

The simulation was carried out by varying the starting month of the installation campaign, to address its sensitivity regarding the accumulated waiting on weather (AWoW). Since the weather dataset uploaded to Shoreline had to be continuous and some recordings were missing, the starting month in the simulation will not correspond directly to the actual starting month, but rather be an approximation. The time stamps for data from FINO3 will always correspond directly to the timestamp for data from ERA5.

Table 9 Installation start month sensitivity

	FINO3		**ERA5**	
Start month	**Installation duration**	**AWoW (Hours)**	**Installation duration**	**AWoW (Hours)**
January	557	5423	524	4682
February	540	5002	505	4233
March	525	4708	498	4096
April	542	5148	516	4550
May	550	5337	542	5180
June	543	5182	538	5036
July	567	5724	519	4671
August	573	5862	528	4884
September	590	6231	552	5403
October	616	6682	576	5857
November	597	6250	560	5479
December	569	5671	544	5108

Results of the simulations conducted individually for installation campaign using weather data from ERA5 and FINO3 at different starting months are shown in Table 9.
This gives an average installation duration of 564 days when using FINO3 weather data and 534 days using ERA5 weather data.
The complete installation time for different starting months are plotted in Figure 22.

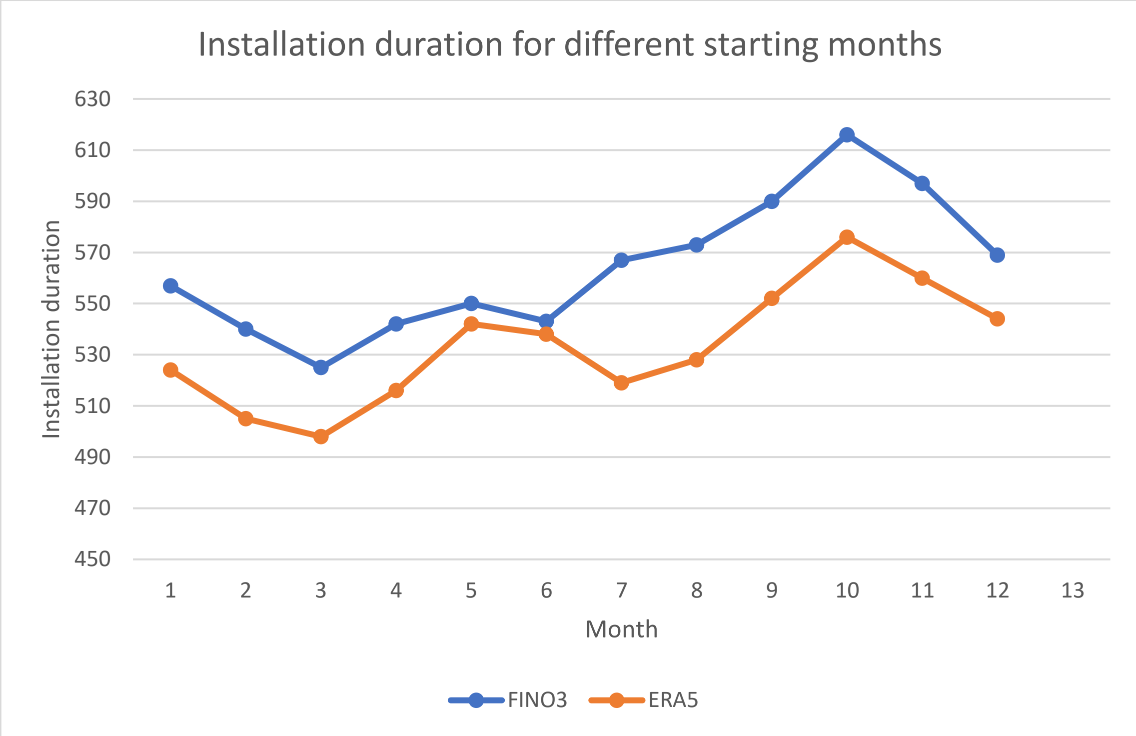

Figure 22 Installation campaign duration for different starting months

The most sensitive part of the installation campaign is previously addressed in chapter 5.3 as being the installation of the turbine blades, demanding low wind speeds and resulting in the lowest number of possible wind weather windows.

In the planning phase of an installation campaign it makes sense to plan the most sensitive operations for the part of the year with the best weather conditions, though the order of operations also must be considered.

The potential value of an intelligent simulation software is shown by helping to schedule the installation process. A variance of 1974 and 1761 hours in AWoW for data from FINO3 and ERA5 respectfully was found, comparing the worst starting month (October) to the best (March).

This leads to a worst-case completion time of 117 % using FINO3 weather data and 116 % using ERA5 weather data, compared to starting at the optimal month.

6 Discussion

In chapter 5 the total installation time of a fictive wind farm was found, based on weather input from observational data on the FINO3 location and weather data from the ERA5 reanalysis.
The wind speed data from FINO3 had to be extrapolated using the Power Law for proper comparison with the wind speed data from ERA5. Since the offshore location of FINO3 is dominated by unstable conditions and abnormal wind profiles, the use of a different wind profile for extrapolation could possibly yield more optimal results (Møller, 2019).
The fact that the observations from FINO3 showed an overall higher wave height compared to data from ERA5, in addition to ERA5 having a higher number of wave weather windows, should decrease the installation completion time using ERA5 weather input calculated in chapter 5.

Although the ERA5 had a higher mean value of the wind speed data compared to data from FINO3, a higher number of wind weather windows was found for the different operations using ERA5 wind data.
A reason for this could be the ERA5 data being more averaged out, compared to observations from FINO3 having more peak values that decrease the number of weather windows.

The sensitivity of wind speed and wave height limitations and operation duration on the project installation time is a factor that could further be investigated. The comparison could also be conducted at other geographic locations offshore with access to observational weather data, such as for example the FINO1 or FINO2 research platforms.

6.1 Current research of the ERA5 reanalysis in other publications

(Ramon, Lledó, Torralba, Soret, & Doblas-Reyes, 2019) performed a study comparing five large global reanalysis datasets to find the one best suited to represent wind speeds at turbine hub height. ERA5, ERA-Interim, the Japanese 55-year Reanalysis (JRA55), the Modern Era Retrospective Analysis for Research and Applications-2 (MERRA2), and the National Centres for Environmental Prediction (NCEP)/National Centre for Atmospheric Research

(NCAR) Reanalysis 1 (R1) was investigated and evaluated against 77 observational towers spread globally. This study concluded that the ERA5 dataset produced the best estimates of near-surface wind speed and variability at hub heights.

As for the ERA5 wave height estimation, a study was performed assessing the performance of ERA5 wave data in a swell dominated region (Bruno, Molfetta, Totaro, & Mossa, 2020).
The study was based on observed wave data collected offshore of the southern Oman coast in the Western Arabian Sea. It was found that throughout the analysed time span the ERA5 reanalysis showed a tendency to overestimate the wave height in swell dominated conditions and underestimate the wave height in wind wave domination, though the prediction of the wind wave height was highly influenced by the wave developing conditions.

7 Conclusion

As the location of future wind farms tend to move further offshore the planning phase of the installation campaign becomes more crucial.
Intelligent simulation tools are offering great potential in project scheduling but is dependent on reliable weather input for accurate estimates.
ERA5 as one of several global weather reanalysis datasets currently available, offers wave data and hourly estimates of wind speeds at an altitude close to typical hub height.
In this study the wave and wind data from the ERA5 reanalysis dataset is compared to corresponding observational wave and wind data from the FINO3 research facility for the period October 2013 to October 2019.
A fictive wind farm was created to be able to run simulations in the SIMSTALL intelligent simulation tool from Shoreline, representing the installation campaign of 80 monopile turbines at the FINO3 location.

Results show that for both the wave and wind data, the number of available weather windows for installation operations are higher in the ERA5 dataset compared to the observational data from FINO3.

The installation campaign simulation gives a total installation time of 564 days using weather input data from FINO3 and 534 days using weather data from ERA5, as an average of twelve different project starting months.

This result indicates that further research should be conducted for validation of reanalysis data before implementation in installation campaign simulation software.

References

Abdalla, S., Isaksen, L., Janssen, P. A. E. M., & Wedi, N. (2013). Effective spectral resolution of ECMWF

atmospheric forecast models. Retrieved from https://www.ecmwf.int/sites/default/files/elibrary/2013/17358-effective-spectral-resolution-ecmwf-atmospheric-forecast-models.pdf

Asgarpour, M. (2016). 17 - Assembly, transportation, installation and commissioning of offshore wind farms. In C. Ng & L. Ran (Eds.), *Offshore Wind Farms* (pp. 527-541): Woodhead Publishing.

Asgarpour, M., Dewan, A., & Savenije, R. (2014). *ROBUST INSTALLATION PLANNING OF OFFSHORE WIND FARMS*. Paper presented at the International Wind Engineering Conference (IWEC 2014) in Hannover, Germany

Bak, T., & Graham, A. (2015). NORCOWE Reference Wind Farm. In K. Guldbrandsen Frøysa & T. Toft-Eriksen (Eds.), (pp. 38-40).

Beinke, T., Ait Alla, A., & Freitag, M. (2017). Resource Sharing in the Logistics of the Offshore Wind Farm Installation Process based on a Simulation Study. *International Journal of e-Navigation and Maritime Economy*, *7*, 42-54. doi:https://doi.org/10.1016/j.enavi.2017.06.005

Bresesti, P., Kling, W. L., Hendriks, R. L., & Vailati, R. (2007). HVDC Connection of Offshore Wind Farms to the Transmission System. *IEEE Transactions on Energy Conversion*, *22*(1), 37-43. doi:10.1109/TEC.2006.889624

Bruno, M. F., Molfetta, M. G., Totaro, V., & Mossa, M. (2020). Performance Assessment of ERA5 Wave Data in a Swell Dominated Region. doi:https://doi.org/10.3390/jmse8030214

Byrkjedal, Ø., Åkervik, E., & Vindteknikk, K. (2009). Vindkart for Norge Retrieved from https://www.nve.no/media/2470/vindkart_for_norge_oppdragsrapporta10-09.pdf

Chen, Y., & Mukerji, P. (2008). *Weather Window Statistical Analysis For Offshore Marine Operations*. Paper presented at the The Eighteenth International Offshore and Polar Engineering Conference, Vancouver, Canada. https://doi.org/

ECMWF. (2012). The ECMWF Ensemble prediction system. Retrieved from https://www.ecmwf.int/sites/default/files/the_ECMWF_Ensemble_prediction_system.pdf

ECMWF. (n.d-a). Climate reanalysis. Retrieved from https://www.ecmwf.int/en/research/climate-reanalysis

ECMWF. (n.d-b). ENS Mean and Spread. Retrieved from https://confluence.ecmwf.int/display/FUG/ENS+Mean+and+Spread

ECMWF. (n.d-c). Observations. Retrieved from https://www.ecmwf.int/en/research/data-assimilation/observations

EOL. (n.d). Wind Direction Quick Reference. Retrieved from https://www.eol.ucar.edu/content/wind-direction-quick-reference

Equinor. (n.d). Havvind Retrieved from https://www.equinor.com/no/what-we-do/wind.html

FINO3. (n.d-a). Meteorology. Retrieved from https://www.fino3.de/en/research/meteorology.html
FINO3. (n.d-b). Wind farms around FINO3. Retrieved from https://www.fino3.de/en/location/wind-farms.html
FINO. (n.d). FINO – Research platforms in the North Sea and Baltic Sea. Retrieved from https://www.fino-offshore.de/en/
Frøysa, K. G. (2016). *NORCOWE Reference Wind Farm*. https://www.sintef.no/globalassets/project/eera-deepwind2016/presentations/x2_froysa.pdf
Hersbach, H., & Dee, D. (n.d). ERA5 reanalysis in production. Retrieved from https://www.ecmwf.int/en/newsletter/147/news/era5-reanalysis-production
Higgins, P., & Foley, A. (2014). The evolution of offshore wind power in the United Kingdom. *Renewable and Sustainable Energy Reviews, 37*, 599-612. doi:https://doi.org/10.1016/j.rser.2014.05.058
IEA. (2019). *World Energy Outlook 2019*. https://www.nordicenergy.org/wp-content/uploads/2019/12/6.2_12-Dec_14.00-14.30_WEOslides-for-DT-for-COP25-FINAL.pdf
Jakobsen, I. U., & Kallbekken, S. (2020). Parisavtalen. Retrieved from https://snl.no/Parisavtalen
Luo, T., Tian, D., Wang, R., & Liao, C. (2018). Stochastic Dynamic Response Analysis of a 10 MW Tension Leg Platform Floating Horizontal Axis Wind Turbine. *Energies, 11*, 3341. doi:10.3390/en11123341
May, T., Yeap, Y. M., & Ukil, A. (2016). *Comparative evaluation of power loss in HVAC and HVDC transmission systems*.
Myhr, A., Bjerkseter, C., Ågotnes, A., & Nygaard, T. A. (2014). Levelised cost of energy for offshore floating wind turbines in a life cycle perspective. *Renewable Energy, 66*, 714-728. doi:https://doi.org/10.1016/j.renene.2014.01.017
Møller, M. (2019). *Comparing Abnormalities in Onshore and Offshore Vertical Wind Profiles* NTNU,
Obhrai, C., Kalvig, S., & Gudmestad, O. (2012). A review of current guidelines and research on wind modeling for the design of offshore wind turbines. *The 22nd International Ocean and Polar Engineering Conference*, 17-22.
Parker, W. S. (2016). Reanalyses and Observations: What's the Difference? *Bulletin of the American Meteorological Society, 97*(9), 1565-1572. doi:10.1175/bams-d-14-00226.1
Paterson, J., D'Amico, F., Thies, P. R., Kurt, R. E., & Harrison, G. (2018). Offshore wind installation vessels – A comparative assessment for UK offshore rounds 1 and 2. *Ocean Engineering, 148*, 637-649. doi:https://doi.org/10.1016/j.oceaneng.2017.08.008
Ramon, J., Lledó, L., Torralba, V., Soret, A., & Doblas-Reyes, F. J. (2019). What global reanalysis best represents near-surface winds? *Quarterly Journal of the Royal Meteorological Society, 145*(724), 3236-3251. doi:10.1002/qj.3616
Toth, Z., & Buizza, R. (2019). Chapter 2 - Weather Forecasting: What Sets the Forecast Skill Horizon? In A. W. Robertson & F. Vitart (Eds.), *Sub-Seasonal to Seasonal Prediction* (pp. 17-45): Elsevier.
Vis, I. F. A., & Ursavas, E. (2016). Assessment approaches to logistics for offshore wind energy installation. *Sustainable Energy Technologies and Assessments, 14*, 80-91. doi:https://doi.org/10.1016/j.seta.2016.02.001

Copernicus Climate Change Service (C3S) (2017): ERA5: Fifth generation of ECMWF atmospheric reanalyses of the global climate. Copernicus Climate Change Service Climate Data Store (CDS), *January 6 2020*. https://cds.climate.copernicus.eu/cdsapp#!/home

Appendix

Code for extracting weather data from Copernicus Climate Data Storage using online toolbox:

```
import cdstoolbox as ct


variables = {
    'Near-Surface Air Temperature': '2m_temperature',
    'Eastward Near-Surface Wind 10': '10m_u_component_of_wind',
    'Northward Near-Surface Wind': '10m_v_component_of_wind',
    'Sea Level Pressure': 'mean_sea_level_pressure',
    'Sea Surface Temperature': 'sea_surface_temperature',
    'Sea Surface Temperature': 'sea_surface_temperature',
    'Eastward Near-Surface Wind 100': '100m_u_component_of_wind',
    'Northward Near-Surface Wind 100': '100m_v_component_of_wind',
    'Mean wave direction': 'mean_wave_direction',
    'Mean wave period': 'mean_wave_period',
    'Sea surface temperature': 'sea_surface_temperature',
    'Significant height of combined wind waves and swell':
'significant_height_of_combined_wind_waves_and_swell'
}

@ct.input.dropdown('variable', label='Variable', values=variables.keys())
@ct.application(title='ERA5 dataset')
@ct.output.download()
def application(variable):

    data = ct.catalogue.retrieve(
        'reanalysis-era5-single-levels',
        {
            'product_type':'reanalysis',
            'variable': variables[variable],
            'area': [50, 0, 60, 10],
            'year': ['2013', '2014', '2015', '2016', '2017', '2018', '2019'],
            'month': [
                '01', '02', '03', '04', '05', '06',
                '07', '08', '09', '10', '11', '12'
            ],
            'day': [
                '01', '02', '03', '04', '05', '06',
                '07', '08', '09', '10', '11', '12',
                '13', '14', '15', '16', '17', '18',
                '19', '20', '21', '22', '23', '24',
                '25', '26', '27', '28', '29', '30',
                '31'
            ],
            'time': [
                '00:00', '01:00', '02:00', '03:00','04:00', '05:00', '06:00',
                '07:00', '08:00', '09:00', '10:00', '11:00','12:00', '13:00',
                '14:00', '15:00', '16:00', '17:00', '18:00', '19:00','20:00',
                '21:00', '22:00', '23:00'
            ],
        }
    )

    data_loc = ct.geo.extract_point(data, lon=7.16, lat=55.18)
```

```
return data_loc
```

Table 10 Turbine installation vessel

Data	Value
Transit Speed (kn)	11
Dynamic positioning Speed (kn)	2
Dynamic Positioning Time (h)	0.5
Significant wave height jacking limit (m)	2.8
Wind speed crane operation limit (m/s)	20
Monopile Foundation capacity (pieces)	5
Transition piece capacity (pieces)	5
Wind turbine components (sets)	5

Table 11 DTU 10-MW reference wind turbine specifications

Description	Value
Turbine power	10 MW
Rotor orientation configuration	Upwind, 3 blades
Control	Variable speed, collective pitch
Drivetrain	Medium speed, multiple stage gearbox
Rotor, Hub diameter	178.3 m, 5.6 m
Hub height	119 m
Cut-in, Rated, Cut-out wind speed	4 m/s, 11.4 m/s, 25 m/s
Cut-in, Rated rotor speed	6 rpm, 9.6 rpm
Rotor mass	229,000 kg
Nacelle mass	446,000 kg
Tower mass	605,000 kg

Table 12 Operation schedule and duration for installation simulation

Transition Piece

Average transit to Esbjerg

86.54km Average wind farm distance
11.0kn (20.4km/h) Transit speed
4.2h Transit time to wind farm

Average transit between assets

1.60km Average asset distance
5.0kn (9.3km/h) Transit speed
0.17h Transit time between assets

Processes

39h Total All Processes

10h Total Foundation loadout
2.00h Loading X 1
2.00h Loading X 2
2.00h Loading X 3
2.00h Loading X 4
2.00h Loading X 5

6h Total Transit to wind farm
3.00h Seafasten assets
2.00h Jacking down
1.00h Port manoevring
0.00h Transit

0h Total Activate dynamic positioning

5h Total Jacking up
1.00h Positioning
2.00h Preload
2.00h Jack-up

10h Total Foundation installation
3.00h X installation
6.00h X airtight platform and bolting
1.00h Finish work

3h Total Jacking down
1.00h Prepare vessel for jacking down(seafasten)
2.00h Jacking down

0h Total Transit to next asset

5h Total Transit from wind farm
0.00h Transit
1.00h Port manoevring
2.00h Positioning/field move
2.00h Jacking @ Loading Yard

Monopile

Average transit to Esbjerg

86.54km Average wind farm distance
11.0kn (20.4km/h) Transit speed
4.2h Transit time to wind farm

Average transit between assets

1.60km Average asset distance
5.0kn (9.3km/h) Transit speed
0.17h Transit time between assets

Processes

38.5h Total All Processes

10h Total Pile loadout
2.00h Loading P 1
2.00h Loading P 2
2.00h Loading P 3
2.00h Loading P 4
2.00h Loading P 5

6h Total Transit to wind farm
3.00h Seafasten assets
2.00h Jacking down
1.00h Port manoevring
0.00h Transit

0h Total Activate dynamic positioning

5h Total Jacking up
1.00h Positioning
2.00h Preload
2.00h Jack-up

8.5h Total Drive pile
2.00h Upending MP from deck
1.00h Stabbing MP
1.00h Remove slings and place hammer
3.00h Piling
0.500h Remove hammer & place on deck
1.00h Place temporary nav aids

1h Total Drill pile
1.00h Drill pile process

3h Total Jacking down
1.00h Prepare vessel for jacking down(seafasten)
2.00h Jacking down

0h Total Transit to next asset

5h Total Transit from wind farm
0.00h Transit
1.00h Port manoevring
2.00h Positioning/field move
2.00h Jacking @ Loading Yard

DTU 10-MW (Wind Turbine)

Average transit to Esbjerg

86.54km Average wind farm distance
11.0kn (20.4km/h) Transit speed
4.2h Transit time to wind farm

Average transit between assets

1.60km Average asset distance
5.0kn (9.3km/h) Transit speed
0.17h Transit time between assets

Processes

75h Total All Processes

37h Total Wind turbine loadout
2.00h Preparing lifting
3.00h Backloading
1.50h Loading tower 1
1.50h Loading tower 2
1.50h Loading tower 3
1.50h Loading tower 4
1.50h Loading tower 5
2.00h Loading nacelle 1
2.00h Loading nacelle 2
2.00h Loading nacelle 3
2.00h Loading nacelle 4
2.00h Loading nacelle 5
2.50h Loading blades set 1
2.50h Loading blades set 2
2.50h Loading blades set 3
2.50h Loading blades set 4
2.50h Loading blades set 5
2.00h Prepare vessel for transit

6h Total Transit to wind farm
3.00h Seafasten assets
2.00h Jacking down
1.00h Port manoevring
0.00h Transit

0h Total Activate dynamic positioning

5h Total Jacking up
1.00h Positioning
2.00h Preload
2.00h Jack-up

19h Total Wind turbine installation
1.00h Prepare TP
1.00h Prepare lifting
4.00h Full Tower
3.00h Nacelle
2.00h Blade 1
2.00h Blade 2
2.00h Blade 3
4.00h Secure WTG

3h Total Jacking down
1.00h Prepare vessel for jacking down(seafasten)
2.00h Jacking down

0h Total Transit to next asset

5h Total Transit from wind farm
0.00h Transit
1.00h Port manoevring
2.00h Positioning/field move
2.00h Jacking @ Loading Yard